

# Detonation transmission experiments at large scale

Josué Melguizo-Gavilanes<sup>1</sup>, and Andrzej Pekalski<sup>2</sup>

<sup>1</sup> Shell Global Solutions B.V., Energy Transition Campus Amsterdam (ETCA)  
Amsterdam, The Netherlands

<sup>2</sup> Shell Research Limited UK, Shell Center  
London, United Kingdom

## 1 Introduction

When hydrogen ( $H_2$ ) is accidentally released, it forms a flammable cloud. If ignited, the flame consumes the flammable parts of the cloud.  $H_2$ -air flames differ significantly from hydrocarbon flames, for which most safety guidelines are designed.  $H_2$ -air has a wide flammability range (4 – 74%  $H_{2,vol}$ ), high mass diffusivity, and shorter combustion times, leading to higher burning velocities and increased flame wrinkling and turbulence. These properties make  $H_2$ -air clouds highly prone to flame acceleration and detonation, which can generate significant overpressures (15 bar) and cause severe explosions. For hydrocarbons, detonations typically propagate to the lower flammability limit (LFL), allowing for consequence assessment based on this metric. However, the lower detonability limit for  $H_2$ -air is not well-defined and is likely much higher, potentially at least twice the LFL. This value, determined in closed systems like pipes, may not represent real accidental scenarios, as detonation limits depend on boundary conditions (closed vs. open systems). Accurately determining these limits is crucial for preventing and mitigating explosion consequences, ensuring appropriate separation distances to protect facilities and personnel. Small changes in the lower limiting concentration for vapor cloud explosions can significantly impact risk assessments and cost savings for businesses handling  $H_2$  (e.g., electrolyzers, high-pressure tanks, refueling stations).<sup>1</sup> Reliable measurement of the lower detonability limit in open space is therefore essential.

Instead of measuring detonability limits in a controlled, pressurized  $H_2$  release, progress can be made by experimentally determining the lowest concentration at which an established planar  $H_2$ -air detonation can propagate. This involves using two semi-confined compartments with different  $H_2$ -air concentrations.<sup>2</sup> The *donor* compartment, filled with a near stoichiometric mixture, in which a detonation is initiated using high explosives. Once the detonation stabilizes at its steady propagation velocity ( $D_{CJ}$ ), it is transmitted to the *acceptor* compartment, which has a lower  $H_2$  concentration towards the LFL. The  $H_2$  concentration in the *acceptor* can then be gradually reduced until the detonation wave fails, thereby indicating the limiting concentration; a similar approach was used in [1] but in closed tubes at laboratory scale. While the main goal of the experimental campaign was to determine the lower detonability limit for  $H_2$ -air at large open scale, the current paper focuses on characterizing the transmission dynamics near the limit.

<sup>1</sup> distance to  $\%H_{2,vol} = 4$  (LFL) is much longer than, say,  $\%H_{2,vol} = 12$ .

<sup>2</sup> Standard setup mimicking an unconfined cloud in which thin plastic is used to contain the reactive mixture.

## 2 Experimental methodology

Eight large-scale Vapor Cloud Explosion (VCE) tests were conducted at BakerRisk's Box Canyon Test Facility (BCTF) in Kinney County, TX, 160 km west of San Antonio. The 931-hectare facility can handle VCE tests of up to 1000 m<sup>3</sup>.

### 2.1 Test rigs/setup

The tests used two rigs, each 30-m long with a square cross-section (height-to-width ratio of 1:1). The rigs, named "3-m rig" and "5-m rig" based on their dimensions, had a 10-m *donor* section where the detonation wave was initiated using a high-explosive charge, followed by a 20-m *acceptor* section to observe detonation wave propagation (or failure) through a lean H<sub>2</sub>-air mixture. Both sections were covered with a continuous plastic sheet (0.15 mm thick) and separated by an intermediate sheet (0.0381 mm thick), secured with spring wire and lock channels. A photo of the 3-m rig is shown in Figure 1 with the main system components annotated.

Industrial-grade H<sub>2</sub> was supplied from a gas tube trailer to the test rig via schedule 40 pipes. Solenoid valves at six points along the pipeline allowed different sections of the rig to be filled at varying rates and concentrations. Twenty-four venturi outlets inside the rig, positioned at 1/3 and 2/3 of the rig's height, introduced the H<sub>2</sub>-air mixture downward. In the 3-m rig, five 0.61 m diameter brushless fans were mounted to ensure a well-mixed fuel-air mixture, with eight fans used in the 5-meter rig. To initiate the detonation in the *donor* section, four 90-g PETN booster charges were placed 1 m from the end of the *donor*, at 1/4 and 3/4 the height and width of the rig. A "hot abort" system was prepared in case of detonation failure or emergency, using two stainless steel leads inside the Donor to ignite the mixture with 30 kV. A secondary "cold abort" system involved two large axial portable fans to blow air into the rig, reducing fuel concentration and maintaining target levels as needed.

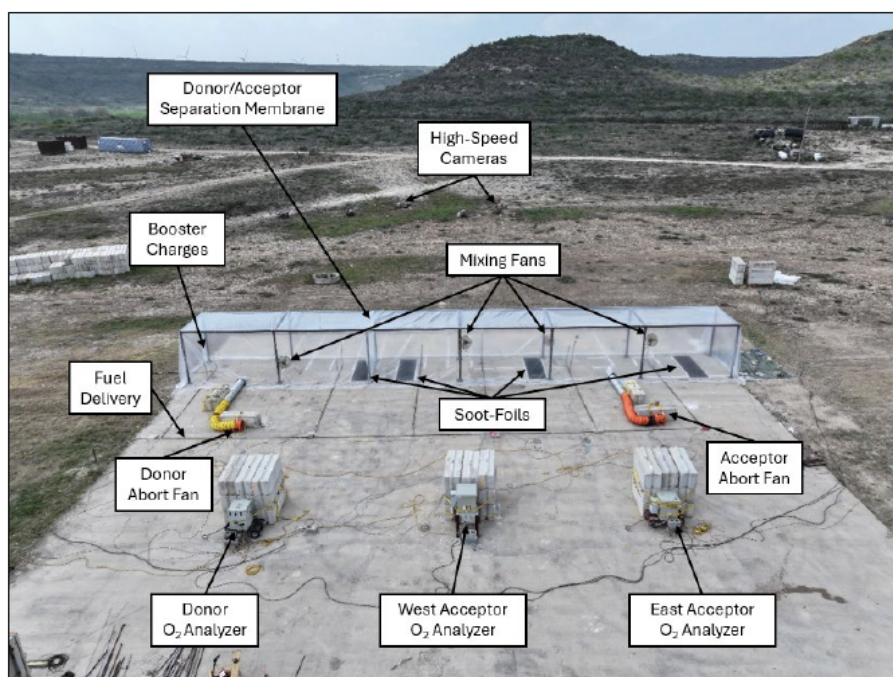


Figure 1: Annotated full-view of experimental setup. The 3-m rig is shown in the picture.

## 2.2 Instrumentation and data acquisition

Three CAI 600P oxygen analyzers were used to indirectly measure fuel concentration in the rig by detecting decreases in oxygen ( $O_2$ ) levels, with a resolution of  $\pm 0.01\%$   $O_2$  by volume. One analyzer measured the *donor* section, while two others, labeled East Acceptor and West Acceptor in Figure 1, measured the *acceptor* section. The *donor* had five sampling points, and the *acceptor* had ten.

Two Phantom VEO 1310 high-speed cameras, capable of recording at least 11 k fps at  $1280 \text{ px} \times 960 \text{ px}$ , were positioned 46 m north of the rig to observe the *donor* and *acceptor* sections separately.

Fifteen PCB CA102B06 high-frequency ICP pressure transducers (PTs), capable of measuring up to 3450 kPa with a sensitivity of 1.45 mV/kPa, were placed along the rig's centerline and connected to a high-speed (1 MHz) DAQ. Four additional sensors were placed along the rig's interior perimeter and connected to a low-speed (100 kHz) DAQ, with two in pinhole and two in flush mount configurations to compare mounting techniques. Ion pins/probes (IPs) were used to measure the reaction front's time of arrival by detecting voltage drops caused by ions in the reaction front. Fifteen IPs were placed near the centerline pressure sensors and separated by a 3.2 mm gap. The optimal voltage across the IPs was found to be 150 V. Prior to each test, the IPs' copper leads were cleaned with 600-grit sandpaper. Figure 2 shows a schematic of the instrumentation arrangement.

Finally, sixteen 102CAB18 PCB gauges were deployed in two parallel lanes perpendicular to the long axis of the rig. The external gauge lanes were centered on the *Donor* and *Acceptor* rig volumes and tied into the low speed (100 kHz) DAQ (not shown).

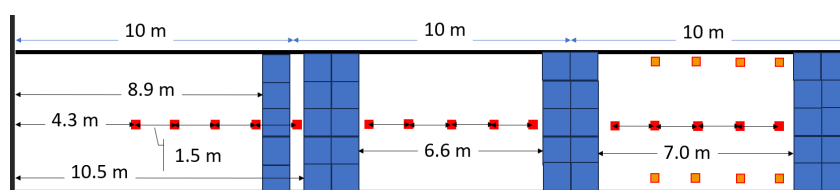


Figure 2: Schematic showing axial locations of pressure transducers, ionization probes and soot foils within rig.

## 2.3 Soot foils

In the 3-m test rig, four  $1.016 \text{ m} \times 3.048 \text{ m}$  soot foils made of 0.8-mm thick, 5052 series aluminum were used, as shown in Figure 1. In the 5-m rig, the *acceptor* soot foils were increased to 5.048 m in length and made of 3.175-mm thick aluminum. The *donor* soot foil thickness was also increased to 3.175 mm, but dimensions remained  $1.016 \text{ m} \times 1.016 \text{ m}$ . The soot foils were placed on plywood to prevent concrete pad impressions, with plywood thicknesses of 0.64 cm for the 3-m tests and 1.9 cm for the 5-m tests. Wilsonart 600 adhesive secured the foil to the plywood, and the assembly was fastened to the concrete floor with steel bar washers and concrete anchors. Drywall mud was used to create a gradual incline at the leading edge to minimize shock wave disruption.

Four soot foils were deployed in each test: (i) Soot Foil #1: centerline of the rig, 0.15 m from the Donor/Acceptor barrier inside the Donor. (ii) Soot Foil #2: leading edge 1 m from the Donor/Acceptor barrier in the Acceptor. (iii) Soot Foil #3: leading edge 9 m from the Donor. (iv) Soot Foil #4: leading edge 19 m from the Donor/Acceptor barrier.

Soot was applied to the panels using a kerosene pool fire, with the panel suspended above the flame with a forklift and moved back and forth until fully covered. Approximately 2.5 L of kerosene per  $\text{m}^2$  was

needed to achieve the desired soot deposition, resulting in more defined detonation cells; darker soot foils resulted in better defined cells.

### 3 Results

#### 3.1 Transmission and marginal propagation dynamics

Figure 3 (left) shows a time sequence of images selected from the high speed videos. The initial moments of propagation, after initiation of the detonation are shown in the bottom frame. The first 10-m comprise the *donor* section whereas the remaining 20-m the *acceptor*. The detonation is observed to propagate steadily in the second half of the *donor* (i.e.  $5 \leq x \text{ [m]} \leq 10$ ) although the front exhibits significant curvature at  $x \sim 7.3 \text{ m}$ ; at the interaction with the donor/acceptor interface the front is almost planar. Shortly after, at around  $x \sim 12.56 \text{ m}$  signs of leading shock-reaction zone decoupling are visible with a very bright region trailing behind a disturbed leading shock along which triple points/transverse waves can be identified. The transmission transient occurs over  $5 - 7 \text{ m}$  (i.e.  $10 < x \text{ [m]} \leq 16$ ) after which the front recovers taking the typical structure described in detail in [2] and references therein for detonation propagation under yielding confinement.

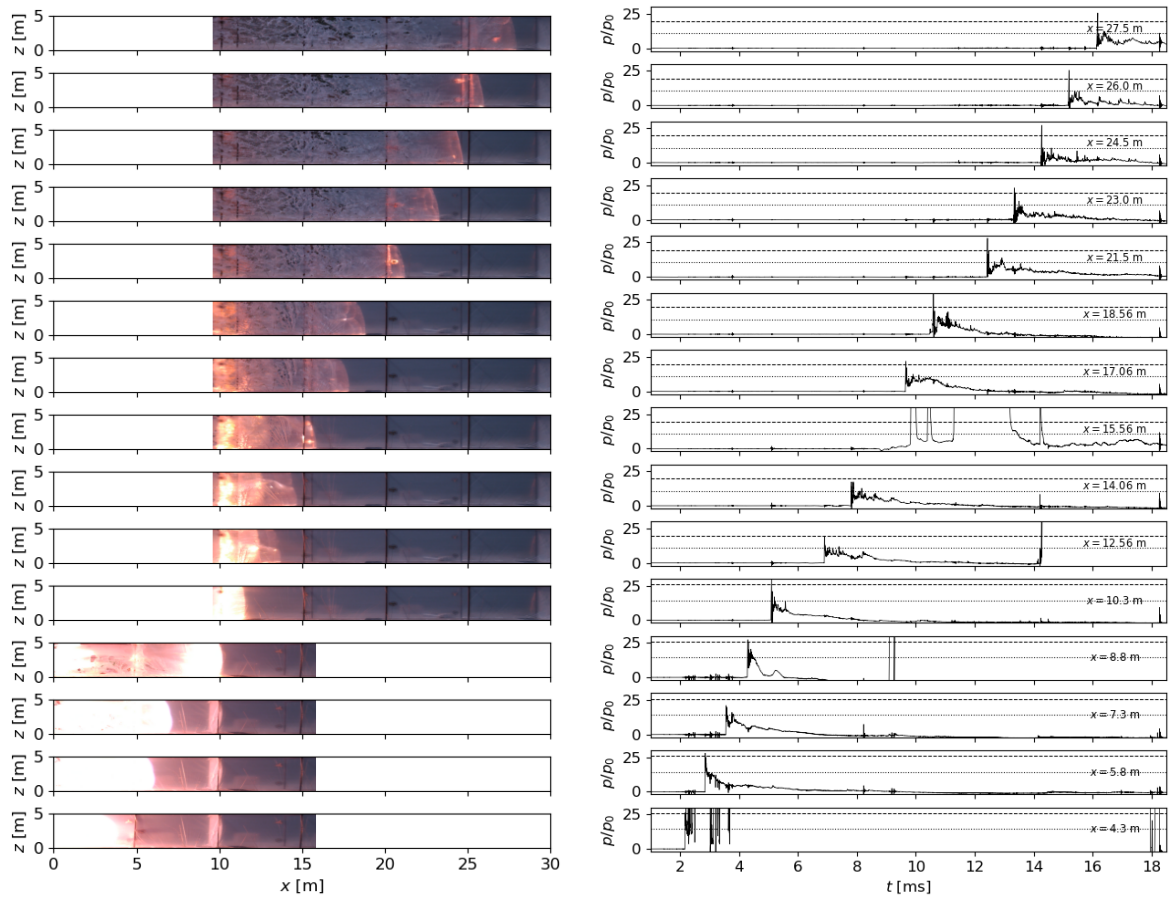


Figure 3: Left: selected video frames corresponding to the moment when the wave passes over the pressure transducer locations. Right: pressure traces along the centerline of the 5-m rig.

Figure 3 (right) shows the high frequency pressure traces (1 MHz) collected along the centerline of the rig; the actual axial locations are displayed on the subplots. Note that the images described above

correspond to the moment the front traverses the pressure transducer locations. The horizontal dashed and dotted lines are the von Neumann (vN) and Chapman-Jouguet (CJ) pressure, respectively, and are plotted as a visual aid for reference. The data at  $x = 15.56$  m is shown for completeness but it is not valid as this PT failed during the test. The data for  $10 < x$  [m]  $\leq 17$  shows the pressure dynamics of the transmission process with a pressure drop indicative of leading shock-reaction zone decoupling as seen in the plots with subsequent recovery for  $18 < x$  [m]  $\leq 30$ . Finally, it is worth mentioning that the traces show the raw data as no averaging has been applied to the signals. This clarification may explain the systematic readings above CJ (and in some instances above vN) recorded throughout the propagation even though velocity deficits are expected to be present. This is quantified in Figure 4.

The high speed videos were postprocessed manually to extract the  $x - t$  (position-time) diagram shown in Figure 4 (left). The slowing down of the wave as it transmits from a  $\text{H}_2$ -air mixture around stoichiometry to a lean  $\text{H}_2$ -air mixture near the detonability limit for this rig size is evident. The transmission transient between  $x = 10 - 15$  m is also visible in the  $x - t$  diagram. The  $u - x$  (velocity-position) diagram computed by numerical differentiation of the position-time data is shown in Figure 4 (right). The dashed lines indicate the CJ-speed ( $D_{\text{CJ}}$ ) whereas the dotted lines the mean front velocities ( $u_{\text{mean}}$ ) in the last 2-m of the *donor*, and last 5-m of the *acceptor*. The figure shows a slight overdrive of the detonation wave ( $u_{\text{mean}}/D_{\text{CJ}} = 1.0087$ ) prior to reaching the donor-acceptor interface. Shortly after the transmission, the leading shock-reaction zone decoupling is quantified by the abrupt drop in front propagation speed to  $u \sim 750$  m/s followed by what appears to be a re-initiation and subsequent stabilization of the wave for  $x > 15$ . The velocity deficit recorded in the last 5-m of the *acceptor* is  $u_{\text{mean}}/D_{\text{CJ}} = 0.93$  similar to those reported close to quenching in recent numerical work [3,4], and in line with the velocity deficits predicted for  $\text{H}_2$  mixtures by the  $D - \kappa$  model (i.e., the turning point of the curves).

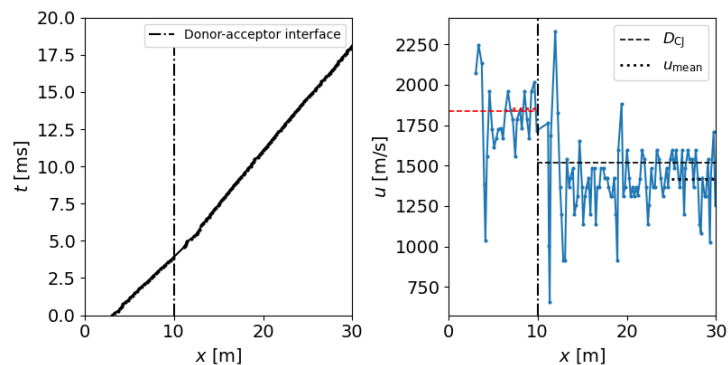


Figure 4:  $x - t$ , and  $u - x$  diagrams showing  $D_{\text{CJ}}$ , and mean front velocities,  $u_{\text{mean}}$ , in the last 2-m of the donor, and 5-m of the acceptor.

### 3.2 Soot foils

To construct Figure 5 the photographs taken at the test site were perspective-corrected, and contrast-enhanced by normalizing their histograms. The postprocessed images were then used to measure cell size samples using ImageJ. The cell size measurements are shown in Figure 5 (right) which display a wide range of length scales present with mean cell sizes ranging from 163 – 230  $\mu\text{m}$ . Overall, the soot foils can be qualitatively classified as being mildly irregular displaying substructures (i.e., cells within cells); there are also larger cells that fade as the edges of the foils are approached. The disappearance of the cellular structure is caused by the expansion fans that are centered at the reactive-inert gas boundary (the edge of the cloud) as the wave propagates. Evidence of re-initiation (very small cells) and partial quenching in some sections of the soot foils are also present. The total area of the soot foils where the

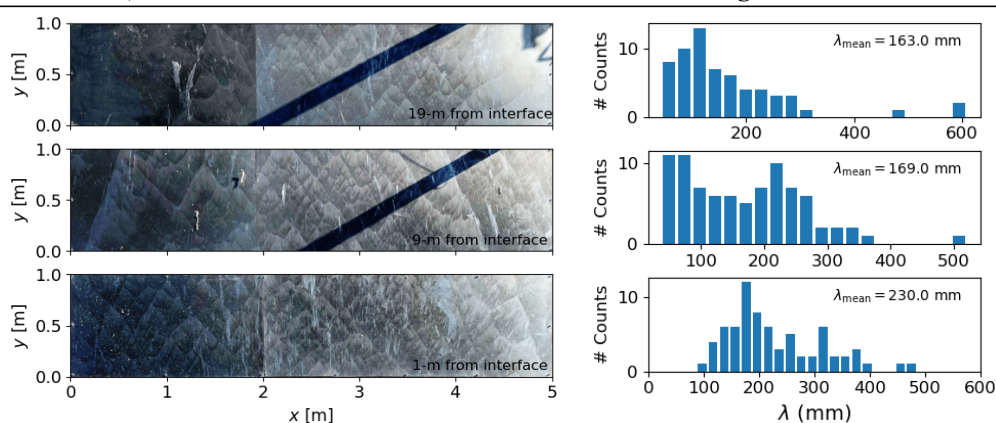


Figure 5: Soot foils collected in the *acceptor* section, and histograms of cell size. Detonation propagation direction from bottom to top.

cellular structure fades increases as the end of the rig is reached ( $x \rightarrow 30$  m). This last observation may suggest that what it is classified as *marginal* propagation herein may indeed be a failure in a longer rig. To the authors knowledge this is the first time soot foils have been collected at this scale.

## 4 Conclusions

A large-scale detonation testing campaign sponsored by Shell and carried out at the Baker Risk Box Canyon testing facility was described in detail. The detonation transmission dynamics for one of the tests performed using the “5-m rig” was analyzed via high-speed videos, pressure traces and soot foils. Results show a transient of 5 – 7 m in length upon interaction with the donor-acceptor interface and subsequent stabilization of the wave with a velocity deficit of  $\sim 7\%$ . The soot foils revealed: (i) a wide range of length scales with signs of re-initiations, and partial quenching as the edges of the foils are approached. (ii) mean cell sizes decreasing from 230 mm to 163 mm as the front reaches the end of the rig. Future work will include a more in-depth analysis of the data including 1-D and 2-D simulations aiming to develop industrially relevant guidance on detonation quenching.

## References

- [1] M. Kuznetsov, S. Dorofeev, A. Efimenko, V. Alekseev, and W. Breitung, “Experimental and numerical studies on transmission of gaseous detonation to a less sensitive mixture,” *Shock Waves*, vol. 7, pp. 297–304, 1997.
- [2] S. Taileb, J. Melguizo-Gavilanes, and A. Chinnayya, “Influence of the chemical modeling on the quenching limits of gaseous detonation waves confined by an inert layer,” *Combustion and Flame*, vol. 218, pp. 247–259, 2020.
- [3] F. Veiga-López, S. Taileb, A. Chinnayya, and J. Melguizo-Gavilanes, “Towards predictive simplified chemical kinetics for hydrogen detonations,” *Combustion and Flame*, vol. 269, p. 113710, 2024.
- [4] H. Watanabe, S. Taileb, F. Veiga-López, J. Melguizo-Gavilanes, and A. Chinnayya, “A simple predictive three-step chemical model for gaseous stoichiometric hydrogen–oxygen detonation quenching,” *Combustion and Flame*, vol. 268, p. 113609, 2024.